Multidisciplinary ⋮ Rapid Review ⋮ Open Access Journal

Received January 30, 2020, accepted March 3, 2020, date of publication March 11, 2020, date of current version March 20, 2020.

Digital Object Identifier 10.1109/ACCESS.2020.2980017

A GaN-Based Wireless Power and Information Transmission Method Using Dual-Frequency Programmed Harmonic Modulation

JIE WU[1], YUEGONG LI[1], NAN JIN[1], (Member, IEEE), WEI DENG[1], HOUJUN TANG[2], AND VÁCLAV SNÁŠEL[3], (Senior Member, IEEE)

[1]Department of Electrical Engineering, Zhengzhou University of Light Industry, Zhengzhou 450002, China
[2]Department of Electrical Engineering, Shanghai Jiao Tong University, Shanghai 200240, China
[3]Department of Computer Science, VŠB-Technical University of Ostrava, 70032 Ostrava, Czech Republic

Corresponding author: Nan Jin (jinnan@zzuli.edu.cn)

This work was supported in part by the National Natural Science Foundation of China under grant U1604136, and in part by the Scientific and Technological Program of Henan Province under grant 202102210090.

ABSTRACT Information transmission is often required in power transfer to implement control. In this paper, a Dual-Frequency Programmed Harmonic Modulation (DFPHM) method is proposed to transfer two frequencies carrying power and information with the single converter via a common inductive coil. The proposed method reduces the number of injection tightly coupled transformers used to transmit information, thereby simplifying the system structure and improving reliability. The performances of power and information transmission, and the method of information modulation and demodulation, as well as the principles of the control, are analyzed in detail. Then a simulation model is set up to verify the feasibility of the method. In addition, an experiment platform is established to verify that the single converter can transfer the power and information simultaneously via a common inductive coil without using tightly coupled transformers.

INDEX TERMS Dual-frequency, full bridge, iteration algorithm, programmed harmonic modulation, wireless power and information transfer.

I. INTRODUCTION

With the development of electronics, the wireless power transfer (WPT) technology has been widely applied for its advantages of convenience and safety [1]–[4]. Nowadays, WPT technology has been used in many fields, such as medical devices, electric vehicles, and so on [5]–[8]. In the field of portable electronics, the wireless charger has become a popular technology. However, in the application scenarios of public areas, the interoperability between the power receiving device and the public charger plays an important role. Additionally, reliable communication between the primary and the secondary side is also an important issue in WPT systems. Therefore, several WPT standards have been set up to increase the interoperability of different devices.

In order to transfer the information while transmitting the power, one idea is to establish an extra physical channel for information transmission by using another module. For example, Radio-frequency (RF) links and other wireless communication devices (such as Bluetooth, Wi-Fi) are common ways employed in many WPT systems for wireless communication [9], [10]. Although these ways can easily realize the simultaneous wireless information and power transfer (SWIPT) and the cost is low, they have lower reliability with an increasing power rating of the WPT system. Besides, the RF systems are easy to be disturbed especially in the complex working environment then cannot operate steadily. Additionally, the extra information module increases the complexity of the system.

The method of using a MOSFET connected parallel at the port of the output is proposed [11]. Only resonant coils are contained in this WPT system. The forward transmission of information is realized by changing the frequency of power transfer. So when the information is transmitted forward, this method makes the circuit work at the expense of resonant, and the transmission efficiency of this system will be affected. Besides, the information backward transmission method based on chopper control and the switching speed of

The associate editor coordinating the review of this manuscript and approving it for publication was Sing Kiong Nguang.

the MOSFET at the secondary side have a direct impact on the information transmission rate.

Another implementation of extra physical channel is multiple inductive links with multiple carriers [12]–[16]. In these methods, power and data are transferred via independent physical channels, where the power carrier is delivered through one inductive link and the data carrier is transmitted via another. In this WPT system, information can be transferred without power transmission. However, this method requires multiple inductive coils that cause extra magnetic interference between the two channels.

In order to reduce the number of coupling devices, the methods of using a common inductive link for power and data transfer have been proposed [17]–[21]. It uses another high-frequency signal generator to produce information flow. At the same time of power transmission, high-frequency information flow and low-frequency power are coupled to the secondary side through a common coil. However, the tight coupling transformers which are used to modulate and demodulate information will influence inevitably the resonance state and efficiency of this system.

In order to realize the wireless power and information transfer with a single inverter and a single inductive link, a GaN-based system with Dual-frequency Programmed Harmonic Modulation (DFPHM) control method is proposed in this paper. In this system, the power is transmitted through the resonant tank without affecting the information transmission. The detailed mathematical model of the proposed multi-frequency system is presented and analyzed in subsequent sections.

This paper is organized as follows. Section II analyzes the principle of the DFPHM. Section III and Section IV discuss the principle of information and power transfer, respectively. The simulation and experimental results are given in Section V. Section VI draws the conclusion.

II. DFPHM PRINCIPLE

For many resonant-type converters used in WPT applications, the transmitter generates single frequency of square waveforms for power transfer. There is only one frequency wave in the circuit. According to the Shannon Theorem, it cannot transfer information with only one frequency. Then, at least two frequencies should be applied to transfer the power and information simultaneously. This paper proposes a control method based on DFPHM, where two frequencies are generated simultaneously and controlled for power supply and information communication via an inductive coil with a full-bridge converter.

As shown in Fig. 1, the dual-frequency inverter generates two frequencies wave by controlling the switching angles of a periodic pulse train of the full control devices. Fig. 1 shows the schematic diagram of full-bridge output voltage under this control method. The synthetic frequency is combined with the two frequencies which are output from the same inverter at the same time. In this study, a fundamental frequency of 26.8 kHz for power transfer and its 37th harmonic

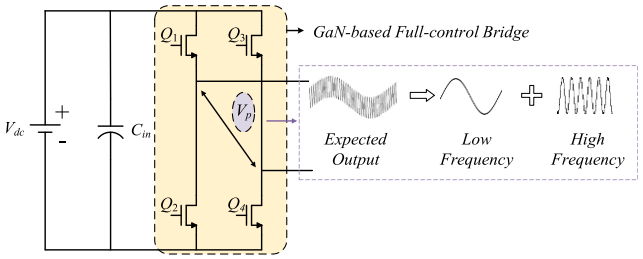

FIGURE 1. The topology of the dual-frequency full bridge inverter.

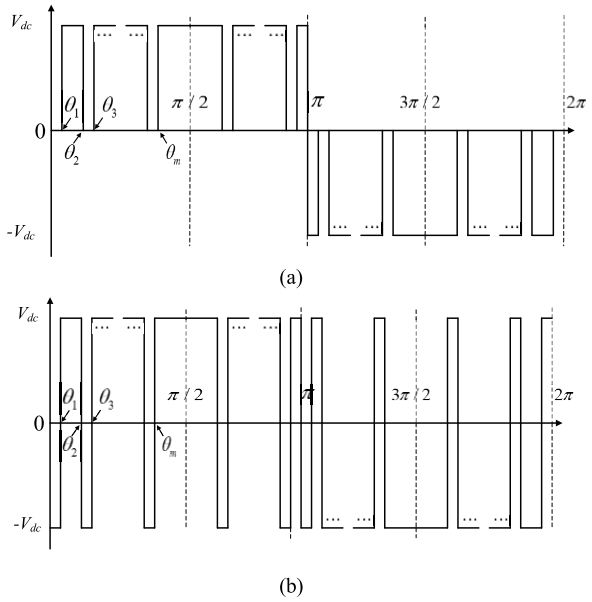

FIGURE 2. The waveform of the DFPHM. (a) The unipolar DFPHM. (b) The bipolar DFPHM.

of 991.6 kHz for information transfer are selected as outputs.

The method that generates the two frequencies is to calculate switching angle consequence of a periodic pulse train to obtain the desired harmonics. Through the control of pulse signals, it remains the desired frequencies and eliminates the other harmonics. The pulse signals can be generated by unipolar modulation or bipolar modulation, as shown in Fig. 2.

The output voltage of the converter obtains two frequencies that vary switching frequency and duty cycle in every switching period, which is different from the original PWM modulation that controls only the fundamental frequency of the output waveform. Fig. 2 (a) shows the waveform of the output voltage with two frequencies. The Fourier expansion of this quarter symmetric unipolar waveform can be expressed as

$$v(\omega t) \sum_{n=1,3,5,\ldots}^{\infty} \frac{4V_{dc}}{n\pi} [\cos(n\theta_1) - \cos(n\theta_2) + \cos(n\theta_3) - \cdots + \cos(n\theta_m)] \cdot \sin(n\omega t) \quad (1)$$

Because of the symmetry of the waveform, those equations contain only even harmonics. Then, the nonlinear equations

of unipolar modulation from (1) is

$$\begin{cases} \cos\theta_1 - \cos\theta_2 + \cdots + \cos\theta_m = \dfrac{\pi}{4} \cdot \dfrac{V_{LF}}{V_{dc}} \\ \cos 3\theta_1 - \cos 3\theta_2 + \cdots + \cos 3\theta_m = 0 \\ \cdots\cdots \\ \cos k\theta_1 - \cos k\theta_2 + \cdots + \cos k\theta_m = \dfrac{k\pi}{4} \cdot \dfrac{V_{HF}}{V_{dc}} \\ \cdots\cdots \\ \cos(2n-1)\theta_1 - \cos(2n-1)\theta_2 + \cdots + \cos(2n-1)\theta_m = 0 \end{cases} \tag{2}$$

where each equation of this system represents the necessary condition of switching angle consequence for modulating a specific harmonic. The V_{dc} is the input DC voltage of the inverter. V_{LF} is the selected amplitude of the frequency for the power transmitter. V_{HF} is the selected amplitude of the frequency for the information transfer.

In this case, the fundamental frequency 26.8 kHz is for power transfer. The 37th harmonic 991.6 kHz is selected for information transfer. The other harmonics are set to zero.

The value of k is set to 37, then its 39th harmonic exists in the circuit. In order to reduce this impact and achieve better results, n is set to 20. So the updated equations are as follows,

$$\begin{cases} \cos\theta_1 - \cos\theta_2 + \cdots + \cos\theta_m = \dfrac{\pi}{4} \cdot \dfrac{V_{LF}}{V_{dc}} \\ \cos 3\theta_1 - \cos 3\theta_2 + \cdots + \cos 3\theta_m = 0 \\ \cdots\cdots \\ \cos 37\theta_1 - \cos 37\theta_2 + \cdots + \cos 37\theta_m = \dfrac{37\pi}{4} \cdot \dfrac{V_{HF}}{V_{dc}} \\ \cos 39\theta_1 - \cos 39\theta_2 + \cdots + \cos 39\theta_m = 0 \end{cases} \tag{3}$$

Similarly, the waveform of the bipolar DFPHM is also a 1/4 period symmetric as shown in Fig. 2(b). And its Fourier expansion of the quarter symmetric waveform is

$$v(\omega t) = \sum_{n=1,3,5,\ldots}^{\infty} \frac{4V_{dc}}{n\pi} [1 - 2\cos(n\theta_1) + 2\cos(n\theta_2) - 2\cos(n\theta_3) + \cdots + 2\cos(n\theta_m)] \cdot \sin(n\omega t) \tag{4}$$

Then, the equations to be solved of bipolar modulation from (4) are

$$\begin{cases} 1 - 2\cos\theta_1 + 2\cos\theta_2 - \cdots + 2\cos\theta_m = \dfrac{\pi}{4} \cdot \dfrac{V_{LF}}{V_{dc}} \\ 1 - 2\cos 3\theta_1 + 2\cos 3\theta_2 - \cdots + 2\cos 3\theta_m = 0 \\ \cdots\cdots \\ 1 - 2\cos 37\theta_1 + 2\cos 37\theta_2 - \cdots + 2\cos 37\theta_m = \dfrac{37\pi}{4} \cdot \dfrac{V_{HF}}{V_{dc}} \\ 1 - 2\cos 39\theta_1 + 2\cos 39\theta_2 - \cdots + 2\cos 39\theta_m = 0 \end{cases} \tag{5}$$

In (3) and (5), m is set to 20, there are 20 nonlinear equations with 20 switching angles to be solved. Generally, it is difficult to solve the 20 nonlinear equations directly. Therefore, some intelligent algorithms, such as particle swarm optimization or genetic algorithm, are employed to obtain the initial values of these angles. And then, a modified Newton-Raphson iteration algorithm is used to get the final result of these switching angles.

TABLE 1. The solved bipolar 20 switching angles case.

Angles Number	Solved Anglese[a]					
θ_1 to θ_6	4.75	9.05	14.20	18.00	23.41	26.62
θ_7 to θ_{12}	31.82	34.27	38.89	41.04	46.51	48.86
θ_{13} to θ_{18}	55.43	57.73	64.87	67.02	74.50	76.51
θ_{19} to θ_{20}	84.19	86.13	-	-	-	-

[a] $V_{LF} / V_{dc} = 0.6$ and $V_{HF} / V_{dc} = 0.6$.

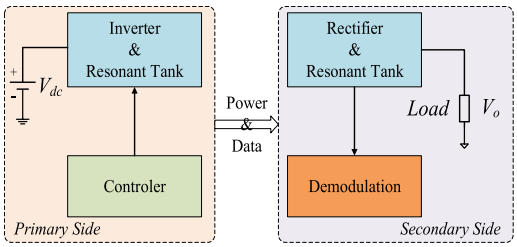

FIGURE 3. The block diagram of the system.

Theoretically, the value of n and m can be taken to any positive integer. As long as the iteration algorithm is convergent, there will exist at least a group of initial values that can satisfy the equations. However, it should be noted that the more switching angles, the harder it is to solve equations. It will definitely increase the computing complexity. Meanwhile, the initial values play an important role for the algorithm convergence.

Using this approach, arbitrary combinations of output frequencies are possible if the higher frequency is integer times of the lower frequency.

For example, when $V_{HF} / V_{dc} = 0.6$, and $V_{LF} / V_{dc} = 0.6$, a set of switching angles are calculated, as shown in Table 1.

III. POWER TRANSFER PRINCIPLE

The basic structure of the WPT system can be divided into SS, SP, PS and PP type according to the connection methods of the primary and secondary LC branches (series and parallel). In this paper, the SS topology is employed as an example of a wireless power and information transfer system.

The block diagram of the system is shown in Fig. 3. The system contains two parts, the primary side and the secondary side share a common resonant channel to transfer the power and information. A full-bridge inverter on the primary side generates simultaneously two different frequencies which are the power transfer frequency and the information transfer frequency. The secondary side is designed to pick up the power and to demodulate the information transferred from the primary side.

The schematic diagram of the circuit is shown in Fig. 4(a), its equivalent circuit model is presented in Fig. 4(b).

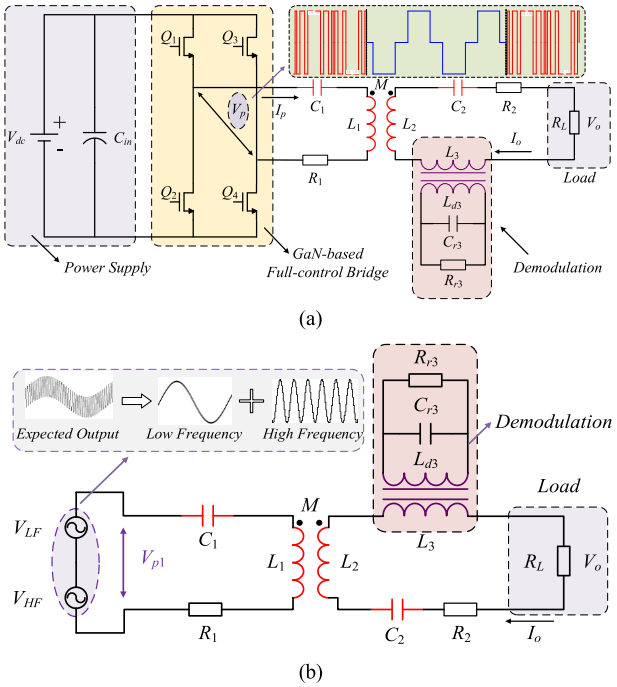

FIGURE 4. The schematic circuit and equivalent circuit using the proposed forward SWIPT method. (a) The schematic circuit; (b) The equivalent circuit model.

The system realizes simultaneous wireless information and power transfer (SWIPT). $Q_1 \sim Q_4$ are the full control devices, which can generate DFPHM signals by controlling the period of the switching angle. For this system, the coupling transformer is plugged in the secondary side to receive the information. In this structure, the information is not injected into the primary side, so the full-bridge inverter should generate two frequencies in the primary side to transfer the information and power to the secondary side simultaneously.

As shown in Fig. 4(b), the V_{LF} and V_{HF} represent the voltage of the two different frequencies for the power and information transfer which are generated from the full-control bridges. Those two frequencies share one inductive coil to transfer the power and information from the primary side to the secondary side. For the communication cell, the R_{r3} and C_{r3} form the resonate cell for the information demodulation. The L_1 and C_1 constitute the resonant tank for the power transfer.

In Fig. 4, V_p and V_{p1} are the output rectangular and equivalent dual-frequency fundamental sine voltage of the inverter, respectively. I_p is the primary output current of the inverter, the I_o represents the current through the load in the secondary side.

As shown in Fig. 4(b), the output voltage of the inverter can be substituted with V_{LF} and V_{HF}. When the low-frequency voltage V_{LF} acts alone, the primary current I_{LF} flows in the circuit, and the load voltage is V_{oLF}. Correspondingly, when the high-frequency voltage V_{HF} acts alone, the primary current I_{HF} flows, and the load voltage is V_{oHF}. According to the superposition principle, the input power can be

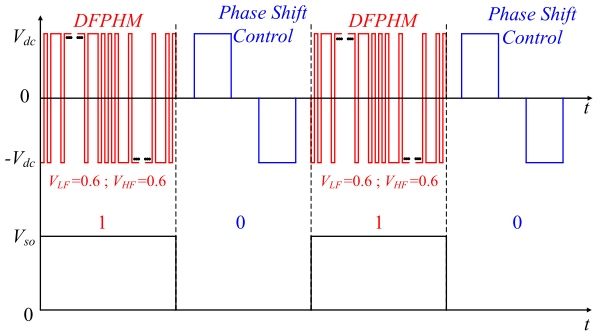

FIGURE 5. The principle of information modulation.

expressed as

$$P_{in} = Re\left(\dot{V}_{LF} \cdot \dot{I}^*_{LF}\right) + Re\left(\dot{V}_{HF} \cdot \dot{I}^*_{HF}\right) \tag{6}$$

The power of R_{r3} and R_L are all from the power supply. If V_{LF} acts alone in this system, the voltage of R_L is V_{oLF} and the power of R_{r3} is P_{LFr3}. If V_{HF} acts alone in this system, V_{oHF} is the voltage of R_L and the P_{HFr3} is the power of R_{r3}. The resistor R_2 is ignored to simplify analysis. So the output power P_{out} is

$$P_{out} = V^2_{oLF} \Big/ R_L + P_{LFr3} + V^2_{oHF} \Big/ R_L + P_{HFr3} \tag{7}$$

Considering the resonant frequency of C_{r3} and L_{d3} is the information frequency, P_{LFr3} can be overlooked and only the power of R_L remains if V_{LF} acts alone in this system. Similarly, if there only V_{HF} acts in this system, the value of R_{r3} is hundreds of times larger than R_L, then, P_{HFr3} can be ignored. Besides, the frequency of V_{HF} is much higher than the frequency of V_{LF}, so V_{oHF} is far less than V_{oLF}, then V_{oHF}/R_L remains. Thus the simplified output power is

$$P_{out} \approx V^2_{oLF} \Big/ R_L \tag{8}$$

Therefore, the efficiency of this WPT system is

$$\eta = \frac{V^2_{oLF}/R_L}{Re(\dot{V}_{LF}\dot{I}^*_{LF}) + Re(\dot{V}_{HF}\dot{I}^*_{HF})} \tag{9}$$

IV. INFORMATION TRANSFER PRINCIPLE

A. INFORMATION MODULATION

ASK (Amplitude Shift Keying) modulation mode is employed in information transmission. Adopting the different control strategy of the inverter, such as DFPHM and phase shift control mode, realizes the information modulation. When using the DFPHM control mode, it will generate two frequencies, 26.8 kHz and 991.6 kHz (the 37th harmonic). When applying the phase shift control, there is only one frequency, 26.8 kHz, in the system. The 991.6 kHz is used as carrier frequency. Fig. 5 shows the principle of information modulation. Signal "1" means that the inverter is control based on DFPHM, and signal "0" indicates that the inverter is controlled under the phase shift control method. V_{so} is the output voltage of the information demodulation module.

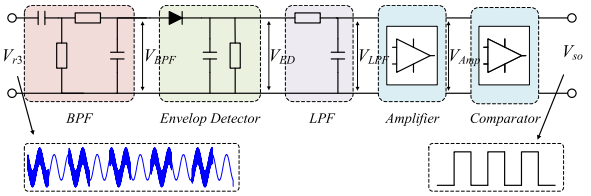

FIGURE 6. The schematic circuit of information demodulation.

B. INFORMATION DEMODULATION

On the secondary side, a demodulation module is designed to pick up the information transmitted from the primary side. This module contains six parts: frequency-selection network, a band-pass filter (BPF), envelop detector (ED), low-pass filter (LPF), amplifier and comparator. The schematic diagram of the demodulation system circuit is shown in Fig. 6.

In Fig. 4, the L_{d3} and C_{d3} make up a frequency-selection network, their resonance frequency is consistent with the information frequency. The V_{r3} is the voltage of R_{r3}. V_{r3} is sent into BPF to eliminate the power frequency and remain the information frequency. The 800 kHz and 1.2 MHz are selected as the band-pass frequency of the BPF.

The output voltage of the BPF, called V_{BPF}, is processed by envelope detector which consists of a diode, capacity and resistance. The envelope detector can monitor the envelope of the signal. The output voltage of envelope detector, V_{ED}, is sent to the LPF. The LPF is used to filter high-frequency signals and ensure data integrity and its cut-off frequency is 100 kHz.

After the third-order passive filtering, the amplitude of the signal is attenuated greatly. To ensure that the output voltage from the LPF, V_{LPF}, can be detected, the amplifier is used. It can magnify the amplitude of V_{LPF}.

The last part of the demodulation unit is the comparator. Setting a corresponding comparison value is necessary for the process of information demodulation. By using this circuits, the information can be demodulated accurately. V_{so} is the output voltage of the demodulated information.

V. SIMULATION AND EXPERIMENT

A. SIMULATION RESULTS

A simulation model is set up to verify the proposed structure. Its parameters are shown in Table 2.

As shown in Fig. 7, a fundamental frequency V_{LF} and its 37th harmonic V_{HF} can be simultaneously generated according to the DFPHM method. The output voltage of the inverter, denoted as V_p, contains two components which are the power and information. The spectrum of V_p is shown in Fig. 8. The result confirms that the proposed method generating the two frequencies in a single inverter is feasible. It can effectively eliminate other harmonics and remain fundamental and higher harmonic rely on the solved angles.

According to the selected amplitudes of V_{LF} and V_{HF}, the values for 20 switching angles are calculated. In this case, the 26.8 kHz is the low frequency (LF) and the 991.6 kHz is the high frequency (HF). The spectrum of the output voltage

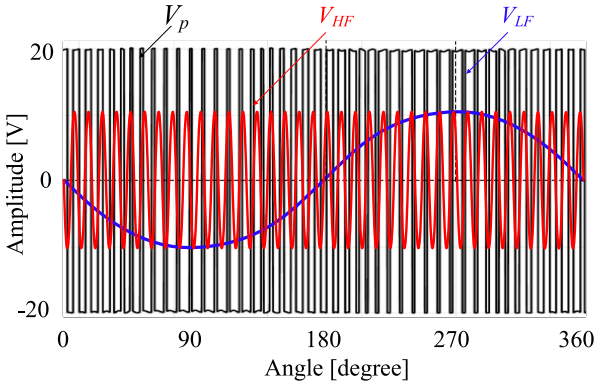

FIGURE 7. The output voltage of the inverter based on DFPHM.

TABLE 2. The parameters of the proposed system.

Variable	Parameter	Value
L_1、L_2	inductance	124μH
M	mutual inductance	36μH
R_1、R_2	the resistance of coil	0.2Ω
C_1、C_2	resonant capacitor	250nF
f	power frequency	26.8 kHz
f_d	information frequency	991.6 kHz
V_{in}	primary side voltage	20V
L_3, L_{d3}	couple inductance	4μH
C_{r3}	the capacitor of wave trapper	6.3nF
$Q_1 \sim Q_4$	GaN Systems	GS66516T

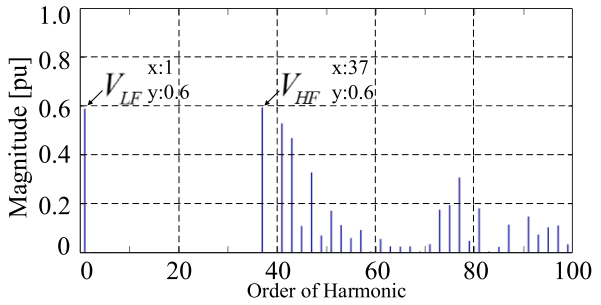

FIGURE 8. The spectrum of the output voltage of the inverter.

of the inverter is shown in Fig. 8. Because the higher-order harmonics whose frequencies are higher than information frequency are not constrained, these components appear in the spectrum. However, Fig. 9 and Fig. 10 indicate that these harmonics do not affect the transmission of power and information.

In this system, the single converter generates the two frequencies by the DFPHM. There are not a lot of interference between power and information. The power of the system can be efficiently transmitted on the shared channel in Fig. 9. The V_{in} is the input voltage and the I_p is the current of the primary side. The V_o and I_o are the load voltage and load current, respectively.

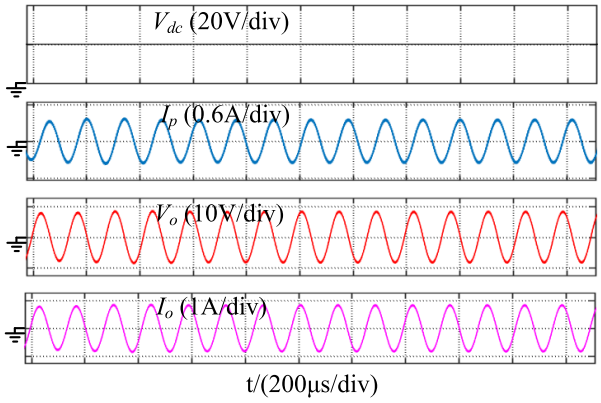

FIGURE 9. The waveform of power transfer.

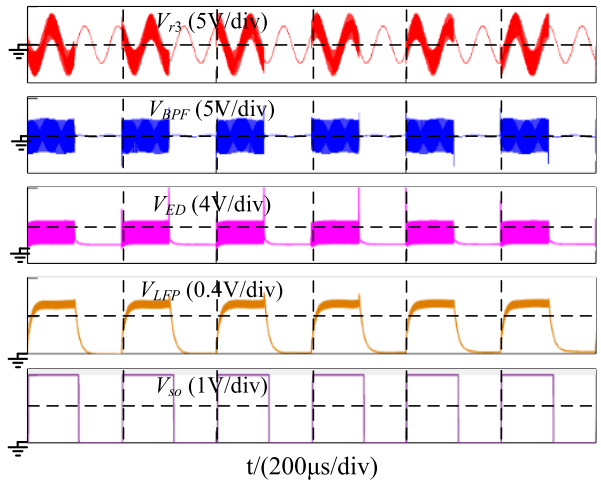

FIGURE 10. The process of information demodulation.

The process of information demodulation is shown in Fig. 10. The single full-bridge inverter generates two frequencies for the information and power transfer through the DFPHM control method. The synthetic waveform uses a single inductive link to complete the simultaneous transmission of power and information. On the secondary side, the close-coupled transformer and compensation capacitor form a resonance cell to receive information frequency. V_{r3} is the voltage of R_{r3}, respectively. Then, the wave is sent into BPF to amplify the gain of the information frequency and reduce the amplitudes of other frequencies. V_{BPF} is the waveform that sent to the envelop detector which is used to detect the magnitude of the voltage. Then another low-pass filter is applied to further diminish high-frequency noise. V_{LPF} is the output voltage of the low-pass filter. The demodulated information is obtained as shown in V_{so}, which is in accordance with the initial information.

B. EXPERIMENTAL RESULTS

The experimental platform is constructed to verify the proposed method as shown in Fig. 11. The full control inverter consists of two half bridges. The full-control bridge inverter is controlled by FPGA. Because of the high switching

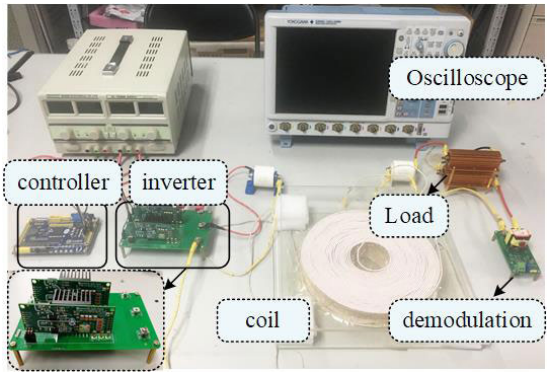

FIGURE 11. The experimental platform of the proposed WPT system.

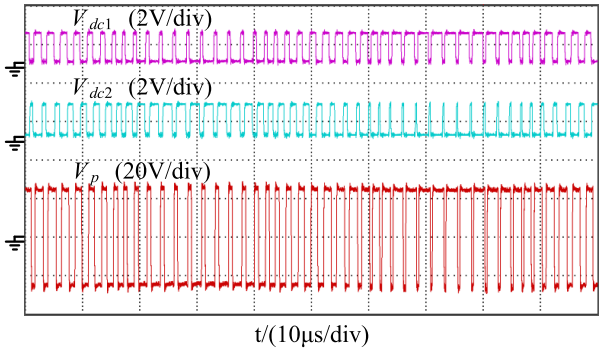

FIGURE 12. The waveform of the gate drive signal and the output voltage of the inverter based on DFPHM. V_{dc1} is the diver signals of Q_1 and Q_4. V_{dc2} is the diver signals of Q_2 and Q_3. V_p is the input voltage.

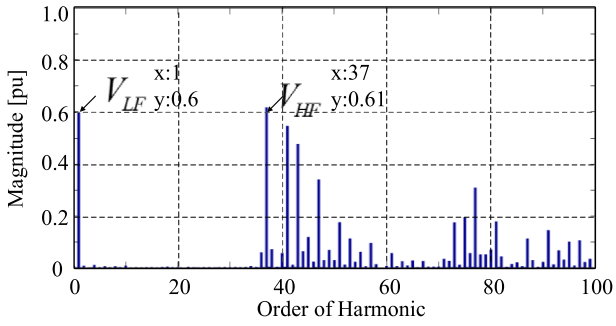

FIGURE 13. The spectrum of the output voltage of the inverter based on DFPHM.

frequency, The GaN-based MOSFET are used as switching chips considering the high switching frequency.

Fig. 12 shows the gate drive signals of the DFPHM. In this control method, the control signals of the switch tube on the same leg are complementary and the control signals of the different leg are the same, which means that the signal of the Q_1 and Q_4 are the same as shown in V_{dc1}, the control signals of Q_2 and Q_3 are the same as shown in V_{dc2}. The V_p is the output voltage of the full-control bridge.

Fig. 13 shows the harmonic components of V_p. According to the results of the experiments, the fundamental frequency and the 37th harmonic frequency got remained. According to

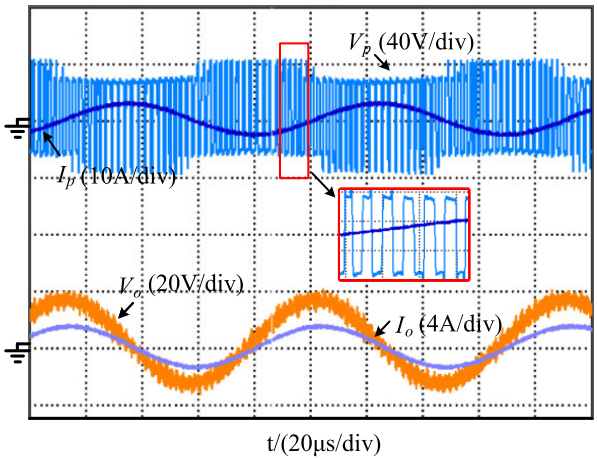

FIGURE 14. The waveform of power transfer in the primary side and secondary side.

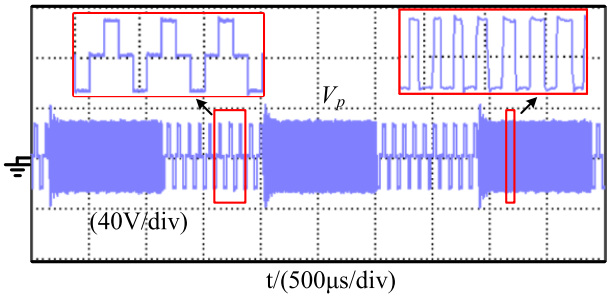

FIGURE 15. The waveform of the inverter based on the DFPHM and phase shift control method.

Fig. 13, it is clear that the DFPHM method can effectively eliminate the target harmonics.

Fig. 14 verifies the proposed idea of DFPHM method. The V_p is the output voltage of the full control bridge. The I_p is the output current of the inverter. In the control strategy of the DFPHM, the power can transmit to the secondary side through the inductive coil to realize the wireless power transfer. At the secondary side, the load voltage and current are represented by V_o and I_o, respectively.

Fig. 15 shows a hybrid control strategy which combines the DFPHM and the phase shift control strategy together to transfer power and information simultaneously. The waveform is also the output voltage of the full control bridge.

According to Fig. 15, the DFPHM is implemented intermittently. Phase shift control is used to keep power transfer without information transmission.

In order to verify that the proposed control strategy can realize the wireless power and information transfer, other experiments are implemented. The results of the experiments are shown as Fig. 16. The dense part means the DFPHM control and the other sparse parts are the phase shift control. The results show that voltage and the currents are in the same phase. The power can be transmitted from the primary side to the secondary side.

Fig. 17 shows the information demodulation process. The waveform of V_{r3} contains the information frequency and

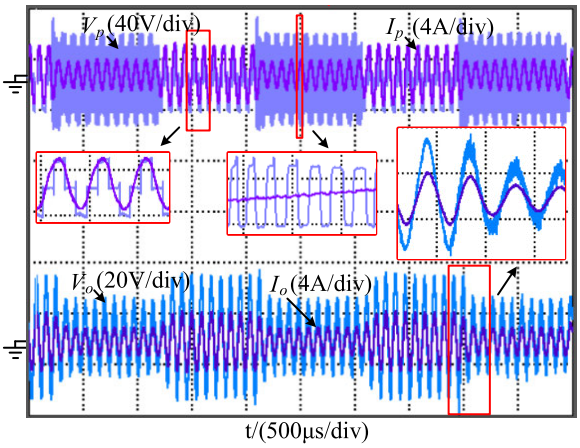

FIGURE 16. The waveform of power transfer based on DFPHM and phase shift control method.

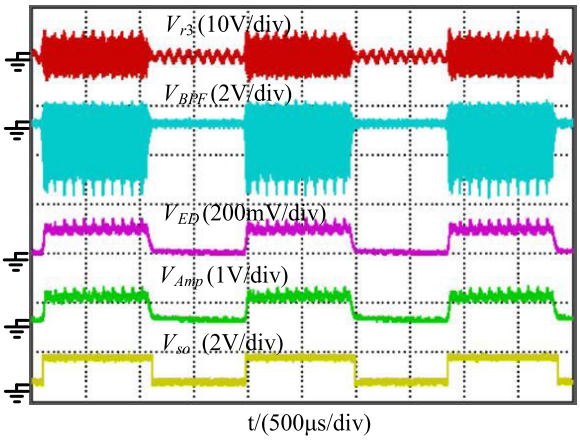

FIGURE 17. The process of the information demodulation.

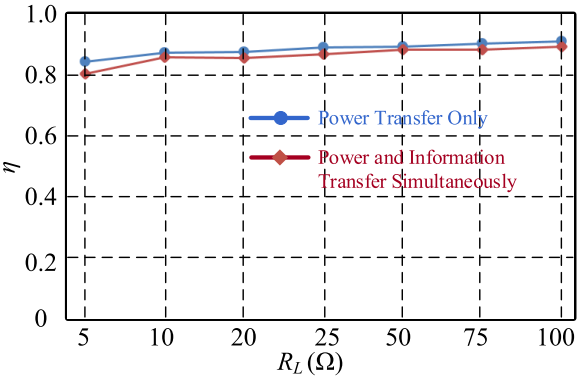

FIGURE 18. The comparison of system efficiency under different loads when only electric energy is transmitted and when electric energy and information are transmitted at the same time.

power frequency. The V_{BPF} is the waveform after the BPF. Its purpose is to amplify the gain of the information frequency and reduce the amplitudes of other frequencies. The V_{ED} is the output voltage of the envelop detector. It detects the amplitude of the wave after the BPF. Because the envelop detector has the advantage of the low costs and easy implementation, it is widely used in signal demodulation. Then the waveform

is sent to another LPF to eliminate high-frequency noise. V_{Amp} is the output voltage of amplifier. Finally, the signal can be obtained by comparator. As shown in Fig. 17, V_{so} is the demodulated information, which is consistent with the initial signal.

In this WPT system, the energy for power transfer and information transmission comes from the total input power of the system. As a result, it is necessary to know that whether information transmission will affect the efficiency of this system when power is being transferred. A series of experiments are carried out where the V_{dc} remains 48V.

Fig. 18 illustrates the comparison of system efficiency under different loads when only electric energy is transmitted and when electric energy and information are transmitted at the same time. Also, when information is transmitted, power transmission is not affected very much.

VI. DISCUSSION AND CONCLUSION

In this paper, a method of the control method to generate two different frequencies based on a single inverter is proposed to realize the simultaneous wireless information and power transfer. The structure of this WPT system is simple and only uses an inductive coil. The results of the simulation and experiment prove the feasibility of the proposed method. Although, in this paper, only the forward transmission of information is analyzed, this structure can be extended to the bidirectional information transmission. In the following research, the full duplex information transmission under this structure will be focused on and verify its feasibility.

REFERENCES

[1] D. T. Garcia, J. Vazque, and S. P. Roncero, "Design, implementation issues and performance of an inductive power transfer system for electric vehicle chargers with series-series compensation," *IET Power Electron.*, vol. 8, no. 10, pp. 1920–1932, Oct. 2015.

[2] D. Ahn and S. Hong, "Wireless power transmission with self-regulated output voltage for biomedical implant," *IEEE Trans. Ind. Electron.*, vol. 61, no. 5, pp. 2225–2235, May 2014.

[3] V. J. Brusamarello, Y. Braga Blauth, R. de Azambuja, I. Müller, and F. R. de Sousa, "Power transfer with an inductive link and wireless tuning," *IEEE Trans. Instrum. Meas.*, vol. 62, no. 5, pp. 924–931, May 2013.

[4] Y. Yao, Y. Wang, X. Liu, H. Cheng, M. Liu, and D. Xu, "Analysis, design, and implementation of a wireless power and data transmission system using capacitive coupling and double-sided LCC compensation topology," *IEEE Trans. Ind. Appl.*, vol. 55, no. 1, pp. 541–551, Jan./Feb. 2019.

[5] B. Esteban, M. Sid-Ahmed, and N. C. Kar, "A comparative study of power supply architectures in wireless EV charging systems," *IEEE Trans. Power Electron.*, vol. 30, no. 11, pp. 6408–6422, Nov. 2015.

[6] U. K. Madawala and D. J. Thrimawithana, "A bidirectional inductive power interface for electric vehicles in V2G systems," *IEEE Trans. Ind. Electron.*, vol. 58, no. 10, pp. 4789–4796, Oct. 2011.

[7] T.-C. Yu and C.-L. Yang, "Design and analysis of dual-frequency power amplifier for wireless power and data transfer application," in *Proc. IEEE Wireless Power Transf. Conf. (WPTC)*, Taipei, Taiwan, May 2017, pp. 1–4.

[8] M. Ogihara, T. Ebihara, K. Mizutani, and N. Wakatsuki, "Wireless power and data transfer system for station-based autonomous underwater vehicles," in *Proc. OCEANS MTS/IEEE Washington*, Washington, DC, USA, Oct. 2015, pp. 1–5.

[9] J. C. Schuder, "Powering an artificial heart: Birth of the inductively coupled-radio frequency system in 1960," *Artif. Organs*, vol. 26, no. 11, pp. 909–915, Nov. 2002.

[10] D. J. Thrimawithana, U. K. Madawala, M. Neath, and T. Geyer, "A sense winding based synchronization technique for bi-directional IPT pick-ups," in *Proc. IEEE Energy Convers. Congr. Expo.*, Phoenix, AZ, USA, Sep. 2011, pp. 1405–1410.

[11] J. Wu, C. Zhao, N. Jin, S. He, and D. Ma, "Bidirectional information transmission in SWIPT system with single controlled chopper receiver," *Electronics*, vol. 8, no. 9, pp. 1027–1041, Aug. 2019.

[12] Z. Dou, S. He, J. Wu, N. Jin, Y. Li, and D. Ma, "Bidirectional communication in the inductive WPT system with injected information transmission," in *Proc. 22nd Int. Conf. Electr. Mach. Syst. (ICEMS)*, Harbin, China, Aug. 2019, pp. 1–5.

[13] A. D. Rush and P. R. Troyk, "A power and data link for a wireless-implanted neural recording system," *IEEE Trans. Biomed. Eng.*, vol. 59, no. 11, pp. 3255–3262, Nov. 2012.

[14] R. Mai, Y. Liu, Y. Li, P. Yue, G. Cao, and Z. He, "An active-rectifier-based maximum efficiency tracking method using an additional measurement coil for wireless power transfer," *IEEE Trans. Power Electron.*, vol. 33, no. 1, pp. 716–728, Jan. 2018.

[15] Z. Pantic, K. Lee, and S. M. Lukic, "Multifrequency inductive power transfer," *IEEE Trans. Power Electron.*, vol. 29, no. 11, pp. 5995–6005, Nov. 2014.

[16] S. Afshar, S. M. R. Tousi, and H. Karami, "Wireless power and full-duplex data transfer system using the combination of TDM and FDM through a same inductive link," in *Proc. Iranian Conf. Elect. Eng. (ICEE)*, Mashhad, Iran, May 2018, pp. 1246–1250.

[17] H. W. Zhou, L. P. Sun, and S. Wang, "Resonant model analysis of wireless power transfer via magnetic resonant coupling," (in Chinese), *Electr. Mach. Control*, vol. 20, no. 7, pp. 65–70, Jul. 2016.

[18] G. Wang, P. Wang, Y. Tang, and W. Liu, "Analysis of dual band power and data telemetry for biomedical implants," *IEEE Trans. Biomed. Circuits Syst.*, vol. 6, no. 3, pp. 208–215, Jun. 2012.

[19] K. Nakanishi and M. Sasaki, "Data transmission system using magnetic resonance wireless power transfer," in *Proc. IEEE Wireless Power Transf. Conf. (WPTC)*, Taipei, Taiwan, May 2017, pp. 1–3.

[20] J. Wu, K. Feng, N. Jin, Z. Wu, S. He, X. Liu, and D. Ma, "Information reverse transmission method for bidirectional WPT with dual active bridges," in *Proc. IEEE/CIC Int. Conf. Commun. Workshops China (ICCC Workshops)*, Changchun, China, Aug. 2019, pp. 196–199.

[21] S. V. D. C. de Freitas, A. Maunder, F. C. Domingos, and P. Mousavi, "Method and system for wireless and single-conductor power and data transmission," in *Proc. IEEE Wireless Power Transf. Conf. (WPTC)*, Aveiro, Portugal, May 2016, pp. 1–3.

JIE WU received the M.Eng. degree in electrical engineering from the Hubei University of Technology, Wuhan, China, in 2005, and the Ph.D. degree from the VŠB-Technical University of Ostrava, Czech Republic, in 2012. He worked with the Hubei University of Technology. Since 2017, he has been a Visiting Professor with the SPARK Laboratory, Department of Electrical and Computer Engineering, University of Kentucky, Lexington, KY, USA. He is currently an Assistant Professor with the Zhengzhou University of Light Industry, Zhengzhou, China. He contributed to the ac flux control technology in hybrid excitation machine. His expertise in electric power engineering includes simultaneous wireless information and power transfer, power electronic drives, and electrical machines.

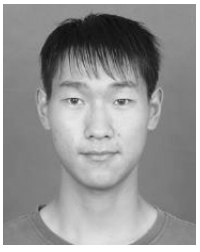

YUEGONG LI was born in Dengzhou, China, in 1994. He received the B.S. degree from the Zhengzhou University of Light Industry, Zhengzhou, China, in 2016, where he is currently pursuing the master's degree.

He was an Electronic Engineer with Guangli Technology Company, Ltd., Zhengzhou. His research interests include simultaneous wireless information and power transfer.

NAN JIN (Member, IEEE) received the B.S. and M.S. degrees in electrical engineering from the Zhengzhou University of Light Industry, Zhengzhou, China, in 2003 and 2007, respectively, and the Ph.D. degree in power electronics and electrical drives from Shanghai Jiao Tong University, Shanghai, China, in 2012.

He was a Visiting Professor with the Department of Electrical Engineering and Computer Science, The University of Tennessee, Knoxville, TN, USA. He is currently a Professor with the Zhengzhou University of Light Industry. He has published more than 50 technical articles in journals and conference proceedings and two books. He holds 12 Chinese patents. His research interests include model predictive control method for power converter, fault diagnosis and tolerant control of power electronics systems, and wireless power transfer. He was a recipient of the 2018 Highlighted Paper Award from the IEEE TPEL.

WEI DENG received the B.S. and M.S. degrees in electrical engineering from Zhengzhou University, Zhengzhou, China, in 2004 and 2007, respectively.

She is currently a Professor with the Zhengzhou University of Light Industry, Zhengzhou. Her current research interests include chaos control, complex network control, wireless power transfer, nonlinear circuit design, and new energy vehicle technology.

HOUJUN TANG received the Ph.D. degree in electrical engineering from Yamagata University, Yamagata, Japan, in 1997.

He is currently a Full Professor with the Department of Electrical Engineering, Shanghai Jiao Tong University, Shanghai, China. His current research interests include wireless power transfer, contactless electric vehicles charging, integration of renewable energy resources, and power electronic drives.

VÁCLAV SNÁŠEL (Senior Member, IEEE) received the master's degree in numerical mathematics from the Faculty of Science, Palacky University, Olomouc, Czech Republic, in 1981, and the Ph.D. degree in algebra and number theory from Masaryk University, Brno, Czech Republic, in 1991.

He is currently a Full Professor with the VŠB-Technical University of Ostrava, Ostrava, Czech Republic. His research and development experience includes more than 30 years in the industry and academia. He works in a multidisciplinary environment involving artificial intelligence, social networks, conceptual lattice, information retrieval, semantic web, knowledge management, data compression, machine intelligence, and nature and bioinspired computing applied to various real-world problems. He has authored or coauthored several refereed journal/conference papers, books, and book chapters.

Dr. Snášel is the Chair of the IEEE International Conference on Systems, Man, and Cybernetics, Czechoslovak Chapter. He also served as an Editor/Guest Editor for a number of journals, such as *Engineering Applications of Artificial Intelligence* (Elsevier), *Neurocomputing* (Elsevier), and *Journal of Applied Logic* (Elsevier).